frontiers | Frontiers in Materials

TYPE Original Research
PUBLISHED 20 September 2022
DOI 10.3389/fmats.2022.977595

Topological states in boron phosphide with zinc-blende structure

Yang Li[1,2]*

[1]Aviation and Automobile School, Chongqing Youth Vocational and Technical College, Chongqing, China, [2]College of Physics, Chongqing University, Chongqing, China

Check for updates

OPEN ACCESS

EDITED BY
Xiaotian Wang,
Southwest University, China

REVIEWED BY
Guangqian Ding,
Chongqing University of Posts and Telecommunications, China,
Gokhan Surucu,
Gazi University, Turkey,
Rabah Khenata,
University of Mascara, Algeria

*CORRESPONDENCE
Yang Li,
liyang_physics@126.com

SPECIALTY SECTION
This article was submitted to Quantum Materials,
a section of the journal
Frontiers in Materials

RECEIVED 24 June 2022
ACCEPTED 17 August 2022
PUBLISHED 20 September 2022

CITATION
Li Y (2022), Topological states in boron phosphide with zinc-blende structure.
Front. Mater. 9:977595.
doi: 10.3389/fmats.2022.977595

The field of topological states in phonon of solids have been rapidly developing in recent years. This work examined the phonon dispersion of a compound Boron Phosphide (BP) with a Zinc-Blende structure via first-principle calculation. The results show that BP is a stable compound in theory and hosts rich topological signatures in its phonon dispersion. Specifically, Weyl and quadratic nodal line states can be found in the acoustic branches, and triple point and quadratic contact triple point can be found in the optical branches. It is hoped that the rich topological states in BP can be imaged by inelastic x-ray scattering or neutron scattering in the near future.

KEYWORDS

topological state, topological phonons, density functional theory, phonon dispersion, optical branch

Introduction

Topological electronic materials have been one of the most active research fields in the past decade. To this date, many types of topological electronic materials (Wang, 2008; Li et al., 2009; Hasan and Kane, 2010; Moore, 2010; Qi and Zhang, 2011; Gao et al., 2016; Tokura et al., 2019; Wang et al., 2020a; Yue et al., 2020), including topological insulators (Hasan and Kane, 2010; Moore, 2010; Qi and Zhang, 2011; Tokura et al., 2019), spin-gapless semiconductors (Wang, 2008; Li et al., 2009; Gao et al., 2016; He et al., 2017; Wang et al., 2020a; Yue et al., 2020; Yang et al., 2021), topological semimetals (Vazifeh and Franz, 2013; Yang et al., 2015; Chang et al., 2016; Liu et al., 2019a; Wang et al., 2020b; Li and Xia, 2020; Lim et al., 2020; Liu et al., 2022a), (Li et al., 2020b; Li et al., 2020c; Li et al., 2020d), and topological superconducting (Chung et al., 2011; Stoudenmire et al., 2011; Sato and Ando, 2017; Zhang et al., 2018; Frolov et al., 2020), have been predicted in theory; some of them are also confirmed in experiments. For example, some three-dimensional (3D) material databases documented tens of thousands of candidates as topological semimetals. In 2019, Zhang *et al.* Zhang et al. (2019a) swept through 39,519 materials in the crystal database and proposed that 8,056 of 39,519 materials have topologically nontrivial properties. In the same year, Vergniory *et al.* Vergniory et al. (2019) performed a high-throughput search of high-quality materials in the Inorganic Crystal Structure Database (ICSD) database and found 4,078 topological semimetals. Tang *et al.* Tang et al. (2019) listed 692 topological semimetals with symmetry-dominated band crossing points around the Fermi level using symmetry indicators. In 2022, Yu et al. Yu et al. (2022)

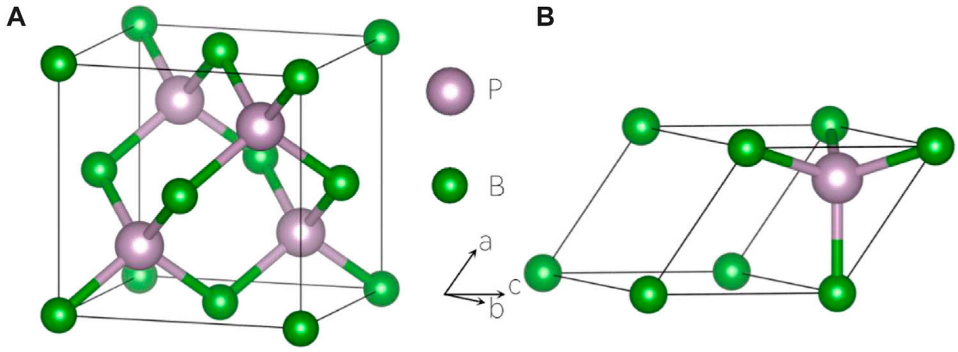

FIGURE 1
(A,B) crystal structure of unit cell and primitive cell of BP.

exhibited an encyclopedia of emergent particles in three-dimensional crystals. They completed a complete list of all possible particles in time-reversal-invariant systems using systematic symmetry analysis.

Very recently, the studies of topological states are intensively generalized to phonons in crystalline materials (Liu et al., 2020a; Chen et al., 2021a; Li et al., 2021). Many realistic solids with diverse topological signatures (Jin et al., 2018a; Jin et al., 2018b; Liu et al., 2019b; Xia et al., 2019; Li et al., 2020a; Liu et al., 2020b; Wang et al., 2020c; Peng et al., 2020; Zheng et al., 2020; Liu et al., 2021a; Wang et al., 2021a; Xie et al., 2021a; Zhou et al., 2021a; Chen et al., 2021b; Liu et al., 2021b; Wang et al., 2021b; Xie et al., 2021b; Zhou et al., 2021b; Liu et al., 2021c; Wang et al., 2021c; Liu et al., 2021d; Wang et al., 2021d; Zheng et al., 2021; Zhong et al., 2021; Ding et al., 2022a; Wang et al., 2022a; Ding et al., 2022b; Liu et al., 2022b; Wang et al., 2022b; Liu et al., 2022c; Yang et al., 2022) are reported via first-principle calculation and symmetry analysis. For example, in theory, solids with Weyl point phonons (Xia et al., 2019; Liu et al., 2020b; Wang et al., 2020c; Liu et al., 2021b), Dirac point phonons (Chen et al., 2021b), nodal chain phonons (Zhou et al., 2021b), nodal box phonons (Zhou et al., 2021b), nodal cage phonons (Ding et al., 2022a; Wang et al., 2022b), and nodal surface phonons (Xie et al., 2021b; Wang et al., 2021d) have been reported. More interestingly, some topological signatures in the phonon spectrum have been confirmed in an experiment with the help of meV-resolution inelastic X-ray scattering. In two consecutive works (Miao et al., 2018; Zhang et al., 2019b), the double Weyl points and the parity-time reversal symmetry-dominated helical nodal lines are realized in the phonon spectrum of FeSi and MoB_2, respectively.

In particular, the coexistence of topological phonons in realistic materials has attracted much attention, such as the coexistence of zero-, one-, and two-dimensional degeneracy phonons (Wang et al., 2021a), hybrid-type nodal-ring and quadratic nodal-line phonons and nodal-net and nodal-link phonons (Zhou et al., 2021b), Dirac nodal line and Weyl nodal line phonons (Wang et al., 2022a). In this work, we focus on a realistic material (Popper and Ingles, 1957), Boron Phosphide (BP), with a Zinc-Blende structure, and study the topological signatures in the phonon dispersion of BP. BP has already been prepared before by the reaction of boron and red phosphorus in an evacuated, sealed silica tube at 1,100°C. BP is with space group F-43m (space group number 216) and contains two atoms, B and P, located at the (0,0,0) and (0.75,0.75,0.75) Wyckoff sites, respectively (see Figure 1A,B). The lattice structure of BP is totally relaxed via first-principle calculation, and the obtained lattice constant is a = b = c = 3.217 Å. To the best of our knowledge, the prosperous topological state has not even been previously reported in the phonon dispersion of BP, and this is the first time to report the topological phonons in the acoustic and optical branches of BP.

Computation methods

The theoretical calculation is performed in the framework of density functional theory (Cohen et al., 2012), which is implemented in the Vienna ab initio Simulation Package (Hafner, 2008). The generalized gradient approximation with Perdew-Burke-Ernzerhof formalism (Perdew et al., 1996) is used for the exchange-correlation energy, and the projector augmented wave method (Blöchl, 1994) is applied for the interactions between the ions and valence electrons. Moreover, a cutoff energy of 500 eV is chosen for the plane wave set, and a Γ-centered k grid of 5 × 5 × 5 is sampled for the Brillouin zone. Based on this optimized lattice of BP, we have computed the phonon dispersion spectrum of 2 × 2 × 2 supercell by the density functional perturbation theory, as implemented within the PHONOPY package (Togo and Tanaka, 2015).

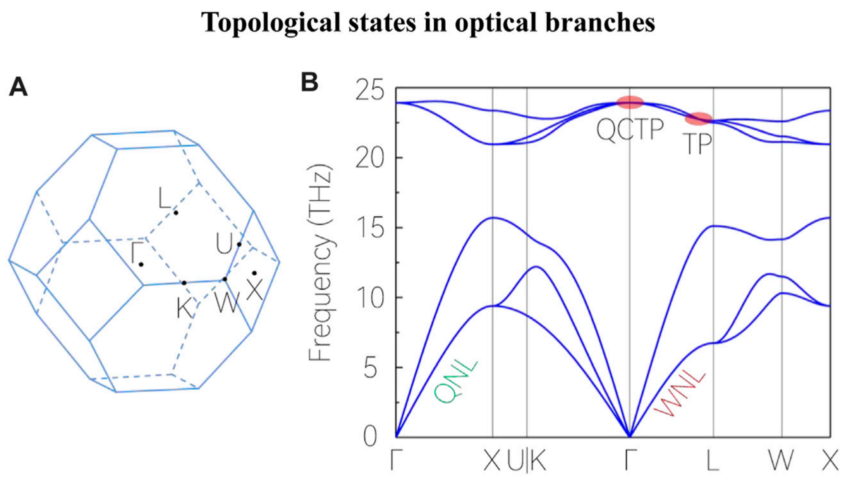

FIGURE 2
(A) Three-dimensional (3D) Brillouin zone (BZ). **(B)** Phonon dispersion of BP.

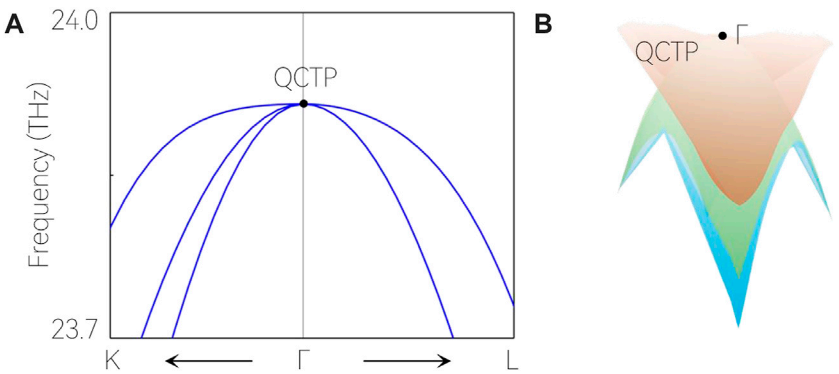

FIGURE 3
(A) Enlarged phonon dispersions of BP along **K** – **Γ** – **L** path. **(B)** 3D plots of QTCP at **Γ**.

Topological states in optical branches

The phonon dispersion of BP along the $\Gamma - X - U|K - \Gamma - L - W - X$ (see Figure 2A) is shown in Figure 2B. BP system contains two atoms, so there should be six branches in the phonon dispersion, i.e., three acoustic branches and three optical branches. As shown in Figure 2B, one finds that there is no imaginary frequency in the phonon dispersion. Moreover, an acoustic-optical branch gap is visible.

For the three optical branches, one finds two crossing points, one is at Γ, and the other one is on $\Gamma - L$ path. The crossing point at Γ is actually a quadratic contact triple point (QCTP). The QCTP is a zero-dimensional (0D) three-fold band degeneracy with a topological charge C = 0. The QCTP only occurs at high-symmetry point in spinless systems, and it features a quadratic energy splitting along any direction in momentum space (see the three-dimensional (3D) plot of the QCTP in Figure 3B). Moreover, the QCTP can split into a doubly degenerate band and a non-degenerate band along the certain high-symmetry line(s) (such as $\Gamma - L$ path in Figure 3A).

As shown in Figure 4A, the crossing point on $\Gamma - L$ path is a triple point (TP) formed by a doubly degenerate band and a non-degenerate band. The 3D plot of the TP on $\Gamma - L$ path is shown in Figure 4B). TP on $\Gamma - L$ path features a linear energy splitting along any direction in momentum space, and is an accidental degeneracy in BZ. We would like to point out that Singh et al. (Singh et al., 2018) also provided evidence of the topological signature in a TP phonon. More interestingly, they (Singh et al., 2018) stated that the appearance of the topological band crossings in phonons could enhance the thermoelectric response in topological metals.

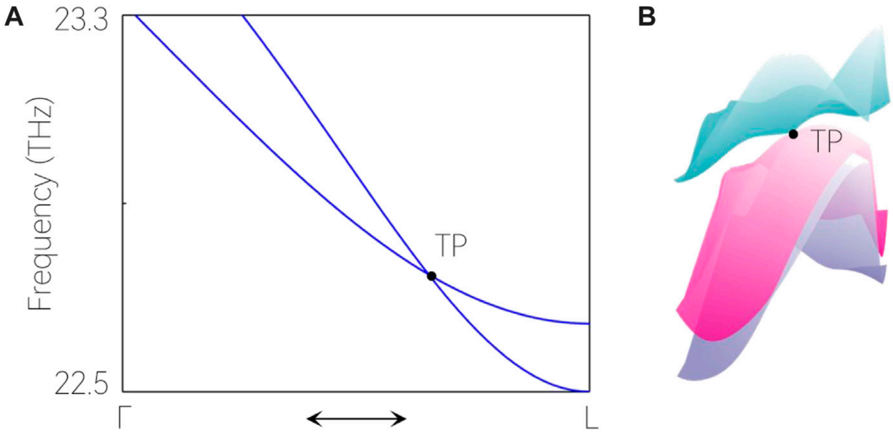

FIGURE 4
(A) Enlarged phonon dispersions of BP along Γ – L path. **(B)** 3D plots of TP on Γ – L path.

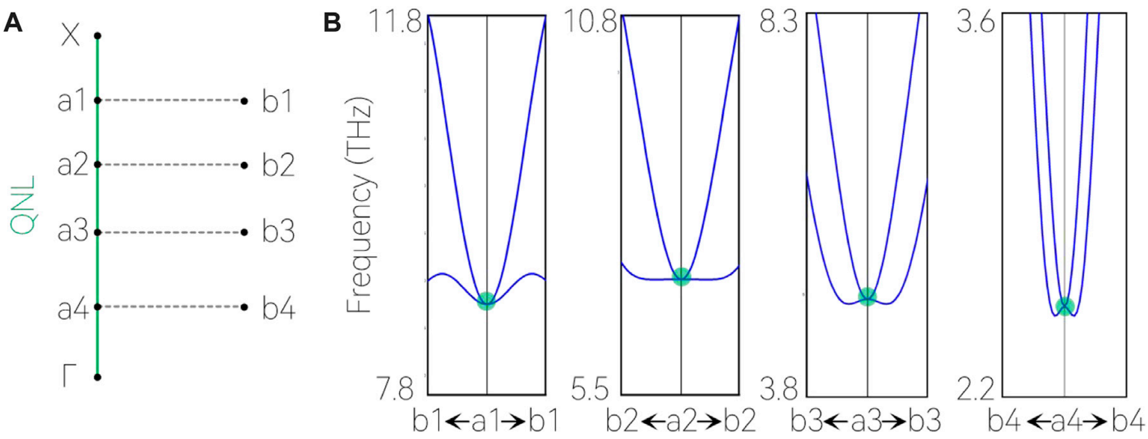

FIGURE 5
(A) Selected symmetry points a1 (0.4, 0.0, 0.4), a2 (0.3, 0.0, 0.3), a3 (0.2, 0.0, 0.2), a4 (0.1, 0.0, 0.1), b1 (0.9, 0.5, 0.4), b2 (0.8, 0.5, 0.3), b3 (0.7, 0.5, 0.2), and b4 (0.6, 0.5, 0.1). **(B)** Enlarged phonon dispersions of BP along the bn-an-bn (n = 1–4) paths.

Topological states in acoustic branches

Then, we come to study the topological states in acoustic branches in BP. As shown in Figure 1C, one finds two doubly degenerate acoustic phonon bands appear along the $\Gamma - X$ and $\Gamma - L$ paths.

The crossing bands along the $\Gamma - X$ path belong to quadratic nodal line (QNL). The QNL is a 1D two-fold band degeneracy and features a quadratic energy splitting in the plane normal to the line. The QNL only occurs along high-symmetry line in 3D BZ. To prove the quadratic energy splitting features of the QNL, we selected some symmetry points, an (n = 1–4) (see Figure 5A), and calculated the phonon dispersions of BP along the bn-an-bn (n = 1–4). The results are shown in Figure 5B. Obviously, a series of crossing points (with green background) with quadratic energy splitting appear on the above *k*-paths.

Actually, the crossing bands along the $\Gamma - L$ path belong to Weyl nodal line (WNL). The WNL is a one-dimensional (1D) two-fold band degeneracy. The WNL features a linear energy dispersion in the plane normal to the line. Moreover, the Berry phase for WNL along the $\Gamma - L$ path equals π, indicating its topologically nontrivial behavior. As shown in Figure 6A, we selected some symmetry points (c1, c2, c3, and c4) on $\Gamma - L$ path, and c1-c4 points equally divided the line $\Gamma - L$. The phonon dispersions of BP along the cn-dn (n = 1–4) are shown

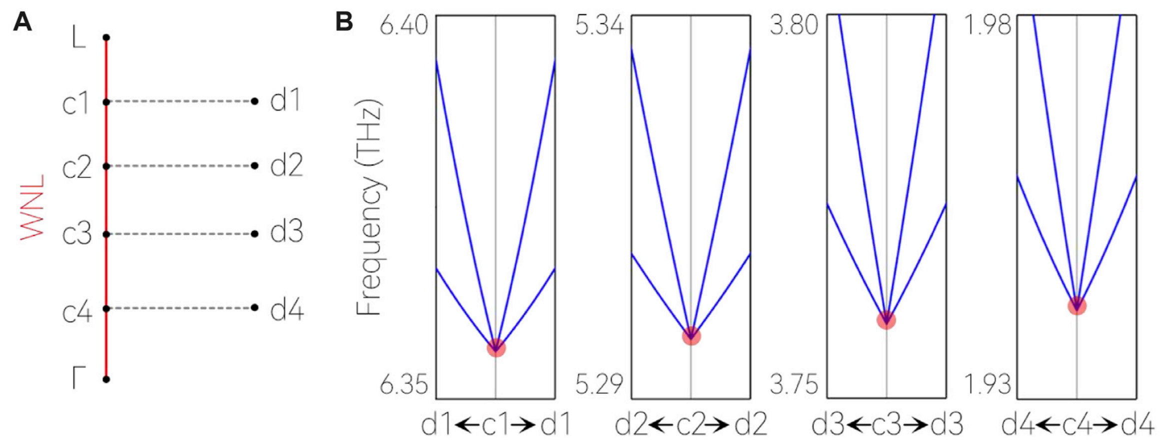

FIGURE 6
(A) Selected symmetry points c1 (0.4, 0.4, 0.4), c2 (0.3, 0.3, 0.3), c3 (0.2, 0.2, 0.2), c4 (0.1, 0.1, 0.1), d1 (0.4, 0.5, 0.4), d2 (0.3, 0.4, 0.3), d3 (0.2, 0.3, 0.2), and d4 (0.1, 0.2, 0.1). **(B)** Enlarged phonon dispersions of BP along the dn-cn-dn (n = 1–4) paths.

in Figure 6B. The band crossings (highlighted by red balls) with a linear band dispersion appear on the selected k paths, i.e., dn-cn-dn (n = 1–4).

Summary

In this work, based on theoretical calculations, we studied the WNL, QNL, TP, and QTCP in the phononic system BP. The acoustic branches form the WNL and QNL and the optical branches form the TP and QCTP. There is a frequency gap between the acoustic and the optical branches. Furthermore, the rich nodal points and rich nodal lines are distributed at different frequency ranges. The WNL phonons along the $\Gamma - L$, the QNL phonons along $\Gamma - X$, the TP on $\Gamma - L$, and the QCTP at Γ are all symmetry-dominated. That is, to say, one can search these topological signatures in phononic systems with space group number 216. However, the TP is accidental degeneracies in 3D BZ; the other three signatures (QNL, WNL, and QCTP) are essential degeneracies in 3D BZ. The reported topological signatures in BP phonon are very clean, and the following technologies, including the inelastic x-ray scattering and neutron scattering, can be selected to image the bulk phonon dispersion of BP in an experiment. Subsequent experimental works are imminent.

Data availability statement

The original contributions presented in the study are included in the article/supplementary material, further inquiries can be directed to the corresponding author.

Author contributions

The author confirms being the sole contributor of this work and has approved it for publication.

Fundings

This work is supported by the Science and Technology Research Program of Chongqing Municipal Education Commission (Grant No. KJZD-K202104101), the Open Project Funding of Theoretical Physics Academic Exchange Platform of Chongqing University (Grant No. 2, in the year of 2021), and the school-level Scientific Research Project of Chongqing Youth Vocational and Technical College (Grant No. CQY2021KYZ03).

Conflict of interest

The author declares that the research was conducted in the absence of any commercial or financial relationships that could be construed as a potential conflict of interest.

Publisher's note

References

Blöchl, P. E. (1994). Projector augmented-wave method. *Phys. Rev. B*, 50(24), 17953, 17979.doi:10.1103/physrevb.50.17953

Chang, G., Xu, S. Y., Zheng, H., Singh, B., Hsu, C. H., Bian, G., et al. (2016). Room-temperature magnetic topological Weyl fermion and nodal line semimetal states in half-metallic Heusler Co2TiX (X= Si, Ge, or Sn). *Sci. Rep.*, 6(1), 38839–9.doi:10.1038/srep38839

Chen, X. Q., Liu, J., and Li, J. (2021). Topological phononic materials: Computation and data. *Innovation*, 2(3), 100134, doi:10.1016/j.xinn.2021.100134

Chen, Z. J., Wang, R., Xia, B. W., Zheng, B. B., Jin, Y. J., Zhao, Y. J., et al. (2021). Three-dimensional Dirac phonons with inversion symmetry. *Phys. Rev. Lett.*, 126(18), 185301, doi:10.1103/physrevlett.126.185301

Chung, S. B., Zhang, H. J., Qi, X. L., and Zhang, S. C. (2011). Topological superconducting phase and Majorana fermions in half-metal/superconductor heterostructures. *Phys. Rev. B*, 84(6), 060510, doi:10.1103/physrevb.84.060510

Cohen, A. J., Mori-Sánchez, P., and Yang, W. (2012). Challenges for density functional theory. *Chem. Rev.*, 112(1), 289–320.doi:10.1021/cr200107z

Ding, G., Sun, T., and Wang, X. (2022). Ideal nodal-net, nodal-chain, and nodal-cage phonons in some realistic materials. *Phys. Chem. Chem. Phys.*, 24(18), 11175–11182.doi:10.1039/d2cp00731b

Ding, G., Zhou, F., Zhang, Z., Yu, Z. M., and Wang, X. (2022). Charge-two Weyl phonons with type-III dispersion. *Phys. Rev. B*, 105(13), 134303, doi:10.1103/physrevb.105.134303

Frolov, S. M., Manfra, M. J., and Sau, J. D. (2020). Topological superconductivity in hybrid devices. *Nat. Phys.*, 16(7), 718–724.doi:10.1038/s41567-020-0925-6

Gao, G., Ding, G., Li, J., Yao, K., Wu, M., and Qian, M. (2016). Monolayer MXenes: Promising half-metals and spin gapless semiconductors. *Nanoscale*, 8(16), 8986–8994.doi:10.1039/c6nr01333c

Hafner, J. (2008). *Ab-initio* simulations of materials using VASP: Density-functional theory and beyond. *J. Comput. Chem.*, 29(13), 2044–2078.doi:10.1002/jcc.21057

Hasan, M. Z., and Kane, C. L. (2010). Colloquium: Topological insulators. *Rev. Mod. Phys.*, 82(4), 3045, 3067.doi:10.1103/revmodphys.82.3045

He, J., Li, X., Lyu, P., and Nachtigall, P. (2017). Near-room-temperature chern insulator and Dirac spin-gapless semiconductor: Nickel chloride monolayer. *Nanoscale*, 9(6), 2246–2252.doi:10.1039/c6nr08522a

Jin, Y. J., Chen, Z. J., Xia, B. W., Zhao, Y. J., Wang, R., and Xu, H. (2018). Ideal intersecting nodal-ring phonons in bcc C8. *Phys. Rev. B*, 98(22), 220103, doi:10.1103/physrevb.98.220103

Jin, Y., Wang, R., and Xu, H. (2018). Recipe for Dirac phonon states with a quantized valley berry phase in two-dimensional hexagonal lattices. *Nano Lett.*, 18(12), 7755–7760.doi:10.1021/acs.nanolett.8b03492

Li, J., Liu, J., Baronett, S. A., Liu, M., Wang, L., Li, R., et al. (2021). Computation and data driven discovery of topological phononic materials. *Nat. Commun.*, 12(1), 1204–1212.doi:10.1038/s41467-021-21293-2

Li, J., Wang, L., Liu, J., Li, R., Zhang, Z., and Chen, X. Q. (2020). Topological phonons in graphene. *Phys. Rev. B*, 101(8), 081403, doi:10.1103/physrevb.101.081403

Li, Y., and Xia, J. (2020). Cubic hafnium nitride: A novel topological semimetal hosting a 0-dimensional (0-D) nodal point and a 1-D topological nodal ring. *Front. Chem.*, 8, 727, doi:10.3389/fchem.2020.00727

Li, Y., Xia, J., Khenata, R., and Kuang, M. (2020). Insight into the topological nodal line metal YB2 with large linear energy range: A first-principles study. *Materials*, 13(17), 3841, doi:10.3390/ma13173841

Li, Y., Xia, J., Khenata, R., and Kuang, M. (2020). Perfect topological metal CrB2: A one-dimensional (1D) nodal line, a zero-dimensional (0D) triply degenerate point, and a large linear energy range. *Materials*, 13(19), 4321, doi:10.3390/ma13194321

Li, Y., Zhang, D., Xia, J., Khenata, R., and Kuang, M. (2020). Cubic ScPd topological metal: Closed nodal line, spin-orbit coupling-induced triply degenerate nodal point–Dirac nodal point transition. *Results Phys.*, 19, 103553, doi:10.1016/j.rinp.2020.103553

Li, Y., Zhou, Z., Shen, P., and Chen, Z. (2009). Spin gapless semiconductor–metal– half-metal properties in nitrogen-doped zigzag graphene nanoribbons. *ACS Nano*, 3(7), 1952–1958.doi:10.1021/nn9003428

Lim, J., Ooi, K. J. A., Zhang, C., Ang, L. K., and Ang, Y. S. (2020). Broadband strong optical dichroism in topological Dirac semimetals with Fermi velocity anisotropy. *Chin. Phys. B*, 29(7), 077802, doi:10.1088/1674-1056/ab928e

Liu, D. F., Liang, A. J., Liu, E. K., Xu, Q. N., Li, Y. W., Chen, C., et al. (2019). Magnetic Weyl semimetal phase in a Kagomé crystal. *Science*, 365(6459), 1282–1285.doi:10.1126/science.aav2873

Liu, D. F., Liu, E. K., Xu, Q. N., Shen, J. L., Li, Y. W., Pei, D., et al. (2022). Direct observation of the spin–orbit coupling effect in magnetic Weyl semimetal Co3Sn2S2. *npj Quantum Mat.*, 7(1), 11–15.doi:10.1038/s41535-021-00392-9

Liu, P. F., Li, J., Tu, X. H., Li, H., Zhang, J., Zhang, P., et al. (2021). First-principles prediction of ideal type-II Weyl phonons in wurtzite ZnSe. *Phys. Rev. B*, 103(9), 094306, doi:10.1103/physrevb.103.094306

Liu, Q. B., Fu, H. H., and Wu, R. (2021). Topological phononic nodal hexahedron net and nodal links in the high-pressure phase of the semiconductor CuCl. *Phys. Rev. B*, 104(4), 045409, doi:10.1103/physrevb.104.045409

Liu, Q. B., Fu, H. H., Xu, G., Yu, R., and Wu, R. (2019). Categories of phononic topological weyl open nodal lines and a potential material candidate: Rb2sn2o3. *J. Phys. Chem. Lett.*, 10(14), 4045–4050.doi:10.1021/acs.jpclett.9b01159

Liu, Q. B., Qian, Y., Fu, H. H., and Wang, Z. (2020). Symmetry-enforced weyl phonons. *npj Comput. Mat.*, 6(1), 95–96.doi:10.1038/s41524-020-00358-8

Liu, Q. B., Wang, Z., and Fu, H. H. (2021). Charge-four weyl phonons. *Phys. Rev. B*, 103(16), L161303, doi:10.1103/physrevb.103.l161303

Liu, Q. B., Wang, Z. Q., and Fu, H. H. (2021). Ideal topological nodal-surface phonons in RbTeAu-family materials. *Phys. Rev. B*, 104(4), L041405, doi:10.1103/physrevb.104.l041405

Liu, Q. B., Wang, Z. Q., and Fu, H. H. (2022). Topological phonons in allotropes of carbon. *Mater. Today Phys.*, 24, 100694, doi:10.1016/j.mtphys.2022.100694

Liu, Y., Chen, X., and Xu, Y. (2020). Topological phononics: From fundamental models to real materials. *Adv. Funct. Mat.*, 30(8), 1904784, doi:10.1002/adfm.201904784

Liu, Y., Zou, N., Zhao, S., Chen, X., Xu, Y., and Duan, W. (2022). Ubiquitous topological states of phonons in solids: Silicon as a model material. *Nano Lett.*, 22(5), 2120–2126.doi:10.1021/acs.nanolett.1c04299

Miao, H., Zhang, T. T., Wang, L., Meyers, D., Said, A. H., Wang, Y. L., et al. (2018). Observation of double Weyl phonons in parity-breaking FeSi. *Phys. Rev. Lett.*, 121(3), 035302, doi:10.1103/physrevlett.121.035302

Moore, J. E. (2010). The birth of topological insulators. *Nature*, 464(7286), 194–198.doi:10.1038/nature08916

Peng, B., Hu, Y., Murakami, S., Zhang, T., and Monserrat, B. (2020). Topological phonons in oxide perovskites controlled by light. *Sci. Adv.*, 6(46), eabd1618, doi:10.1126/sciadv.abd1618

Perdew, J. P., Burke, K., and Ernzerhof, M. (1996). Generalized gradient approximation made simple. *Phys. Rev. Lett.*, 77(18), 3865–3868.doi:10.1103/physrevlett.77.3865

Popper, P., and Ingles, T. A. (1957). Boron phosphide, a III–V compound of zinc-blende structure. *Nature*, 179(4569), 1075–1075.doi:10.1038/1791075a0

Qi, X. L., and Zhang, S. C. (2011). Topological insulators and superconductors. *Rev. Mod. Phys.*, 83(4), 1057, 1110.doi:10.1103/revmodphys.83.1057

Sato, M., and Ando, Y. (2017). Topological superconductors: A review. *Rep. Prog. Phys.*, 80(7), 076501, doi:10.1088/1361-6633/aa6ac7

Singh, S., Wu, Q., Yue, C., Romero, A. H., and Soluyanov, A. A. (2018). Topological phonons and thermoelectricity in triple-point metals. *Phys. Rev. Mat.*, 2(11), 114204, doi:10.1103/physrevmaterials.2.114204

Stoudenmire, E. M., Alicea, J., Starykh, O. A., and Fisher, M. P. (2011). Interaction effects in topological superconducting wires supporting Majorana fermions. *Phys. Rev. B*, 84(1), 014503, doi:10.1103/physrevb.84.014503

Tang, F., Po, H. C., Vishwanath, A., and Wan, X. (2019). Comprehensive search for topological materials using symmetry indicators. *Nature*, 566(7745), 486–489.doi:10.1038/s41586-019-0937-5

Togo, A., and Tanaka, I. (2015). First principles phonon calculations in materials science. *Scr. Mater.*, 108, 1–5.doi:10.1016/j.scriptamat.2015.07.021

Tokura, Y., Yasuda, K., and Tsukazaki, A. (2019). Magnetic topological insulators. *Nat. Rev. Phys.*, 1(2), 126–143.doi:10.1038/s42254-018-0011-5

Vazifeh, M. M., and Franz, M. (2013). Electromagnetic response of Weyl semimetals. *Phys. Rev. Lett.*, 111(2), 027201, doi:10.1103/physrevlett.111.027201

Vergniory, M. G., Elcoro, L., Felser, C., Regnault, N., Bernevig, B. A., and Wang, Z. (2019). A complete catalogue of high-quality topological materials. *Nature*, 566(7745), 480–485.doi:10.1038/s41586-019-0954-4

Wang, H. X., Lin, Z. K., Jiang, B., Guo, G. Y., and Jiang, J. H. (2020). Higher-order weyl semimetals. *Phys. Rev. Lett.*, 125(14), 266804, doi:10.1103/physrevlett.125.266804

Wang, J., Yuan, H., Kuang, M., Yang, T., Yu, Z. M., Zhang, Z., et al. (2021). Coexistence of zero-one-and two-dimensional degeneracy in tetragonal SnO2 phonons. *Phys. Rev. B*, 104(4), L041107, doi:10.1103/physrevb.104.l041107

Wang, J., Yuan, H., Liu, Y., Zhou, F., Wang, X., and Zhang, G. (2022). Hourglass Weyl and Dirac nodal line phonons, and drumhead-like and torus phonon surface states in orthorhombic-type KCuS. *Phys. Chem. Chem. Phys.*, 24(5), 2752–2757.doi:10.1039/d1cp05217a

Wang, J., Yuan, H., Yu, Z. M., Zhang, Z., and Wang, X. (2021). Coexistence of symmetry-enforced phononic Dirac nodal-line net and three-nodal surfaces phonons in solid-state materials: Theory and materials realization. *Phys. Rev. Mat.*, 5(12), 124203, doi:10.1103/physrevmaterials.5.124203

Wang, M., Wang, Y., Yang, Z., Fan, J., Zheng, B., Wang, R., et al. (2022). Symmetry-enforced nodal cage phonons in Th2BC2. *Phys. Rev. B*, 105(17), 174309, doi:10.1103/physrevb.105.174309

Wang, R., Xia, B. W., Chen, Z. J., Zheng, B. B., Zhao, Y. J., and Xu, H. (2020). Symmetry-protected topological triangular Weyl complex. *Phys. Rev. Lett.*, 124(10), 105303, doi:10.1103/physrevlett.124.105303

Wang, R. Y., Chen, Z. J., Huang, Z. Q., Xia, B. W., and Xu, H. (2021). Classification and materials realization of topologically robust nodal ring phonons. *Phys. Rev. Mat.*, 5(8), 084202, doi:10.1103/physrevmaterials.5.084202

Wang, X., Cheng, Z., Zhang, G., Yuan, H., Chen, H., and Wang, X. L. (2020). Spin-gapless semiconductors for future spintronics and electronics. *Phys. Rep.*, 888, 1–57.doi:10.1016/j.physrep.2020.08.004

Wang, X. L. (2008). Proposal for a new class of materials: Spin gapless semiconductors. *Phys. Rev. Lett.*, 100(15), 156404, doi:10.1103/physrevlett.100.156404

Wang, X., Zhou, F., Yang, T., Kuang, M., Yu, Z. M., and Zhang, G. (2021). Symmetry-enforced ideal lanternlike phonons in the ternary nitride Li6WN4. *Phys. Rev. B*, 104(4), L041104, doi:10.1103/physrevb.104.l041104

Xia, B. W., Wang, R., Chen, Z. J., Zhao, Y. J., and Xu, H. (2019). Symmetry-protected ideal type-II Weyl phonons in CdTe. *Phys. Rev. Lett.*, 123(6), 065501, doi:10.1103/physrevlett.123.065501

Xie, C., Liu, Y., Zhang, Z., Zhou, F., Yang, T., Kuang, M., et al. (2021). Sixfold degenerate nodal-point phonons: Symmetry analysis and materials realization. *Phys. Rev. B*, 104(4), 045148, doi:10.1103/physrevb.104.045148

Xie, C., Yuan, H., Liu, Y., Wang, X., and Zhang, G. (2021). Three-nodal surface phonons in solid-state materials: Theory and material realization. *Phys. Rev. B*, 104(13), 134303, doi:10.1103/physrevb.104.134303

Yang, L. X., Liu, Z. K., Sun, Y., Peng, H., Yang, H. F., Zhang, T., et al. (2015). Weyl semimetal phase in the non-centrosymmetric compound TaAs. *Nat. Phys.*, 11(9), 728–732.doi:10.1038/nphys3425

Yang, T., Cheng, Z., Wang, X., and Wang, X. L. (2021). Nodal ring spin gapless semiconductor: New member of spintronic materials. *J. Adv. Res.*, 28, 43–49.doi:10.1016/j.jare.2020.06.016

Yang, T., Xie, C., Chen, H., Wang, X., and Zhang, G. (2022). Phononic nodal points with quadratic dispersion and multifold degeneracy in the cubic compound Ta3Sn. *Phys. Rev. B*, 105(9), 094310, doi:10.1103/physrevb.105.094310

Yu, Z. M., Zhang, Z., Liu, G. B., Wu, W., Li, X. P., Zhang, R. W., et al. (2022). Encyclopedia of emergent particles in three-dimensional crystals. *Sci. Bull.*, 67(4), 375–380.doi:10.1016/j.scib.2021.10.023

Yue, Z., Li, Z., Sang, L., and Wang, X. (2020). Spin-gapless semiconductors. *Small*, 16(31), 1905155, doi:10.1002/smll.201905155

Zhang, P., Yaji, K., Hashimoto, T., Ota, Y., Kondo, T., Okazaki, K., et al. (2018). Observation of topological superconductivity on the surface of an iron-based superconductor. *Science*, 360(6385), 182–186.doi:10.1126/science.aan4596

Zhang, T., Jiang, Y., Song, Z., Huang, H., He, Y., Fang, Z., et al. (2019). Catalogue of topological electronic materials. *Nature*, 566(7745), 475–479.doi:10.1038/s41586-019-0944-6

Zhang, T. T., Miao, H., Wang, Q., Lin, J. Q., Cao, Y., Fabbris, G., et al. (2019). Phononic helical nodal lines with PT protection in MoB2. *Phys. Rev. Lett.*, 123(24), 245302, doi:10.1103/physrevlett.123.245302

Zheng, B., Xia, B., Wang, R., Chen, Z., Zhao, J., Zhao, Y., et al. (2020). Ideal type-III nodal-ring phonons. *Phys. Rev. B*, 101(10), 100303, doi:10.1103/physrevb.101.100303

Zheng, B., Zhan, F., Wu, X., Wang, R., and Fan, J. (2021). Hourglass phonons jointly protected by symmorphic and nonsymmorphic symmetries. *Phys. Rev. B*, 104(6), L060301, doi:10.1103/physrevb.104.l060301

Zhong, M., Liu, Y., Zhou, F., Kuang, M., Yang, T., Wang, X., et al. (2021). Coexistence of phononic sixfold, fourfold, and threefold excitations in the ternary antimonide Zr3Ni3Sb4. *Phys. Rev. B*, 104(8), 085118, doi:10.1103/physrevb.104.085118

Zhou, F., Chen, H., Yu, Z. M., Zhang, Z., and Wang, X. (2021). Realistic cesium fluogermanate: An ideal platform to realize the topologically nodal-box and nodal-chain phonons. *Phys. Rev. B*, 104(21), 214310, doi:10.1103/physrevb.104.214310

Zhou, F., Zhang, Z., Chen, H., Kuang, M., Yang, T., and Wang, X. (2021). Hybrid-type nodal ring phonons and coexistence of higher-order quadratic nodal line phonons in an AgZr alloy. *Phys. Rev. B*, 104(17), 174108, doi:10.1103/physrevb.104.174108